Pathogen intrusion flows in water distribution systems: according to orifice equations

Jesús Mora-Rodríguez, Xitlali Delgado-Galván, Josefina Ortiz-Medel, Helena M. Ramos, Vicente S. Fuertes-Miquel and P. Amparo López-Jiménez

ABSTRACT

Pathogen intrusion may occur in water pipes when negative pressures allow external flows to enter through failures or leaks and then mix with safe water. Based on the Fixed and Variable Area Discharge (FAVAD) theory and the orifice equations, an analysis is proposed to estimate the intrusion flow across defects in pipes considering different types of failure. The equivalent diameter of different round hole failures was considered in order to obtain the dimensions of the split failures that presented the same pressure drop. In addition, experimental scenarios were made with external porous media to model the intrusion flow in buried pipes. An inverse method for the orifice equation is proposed to obtain the intrusion flows generated by the variations of two section failures produced by the pressure drop inside the pipe. The orifice equation properly represents the intrusion flow by adjusting the discharge coefficient. Furthermore, the considerable variations in the failures area with negative pressures should be taken into consideration in the expressions that estimate the intrusion flow.

Key words | buried pipes, failure pipes, FAVAD, physical model

Jesús Mora-Rodríguez
Xitlali Delgado-Galván
Josefina Ortiz-Medel
Geomatics and Hydraulic Engineering Department,
Universidad de Guanajuato,
Av. Juárez No. 77, Centro, 36000 Guanajuato,
Mexico

Helena M. Ramos (corresponding author)
Civil Engineering Department and CEris,
Instituto Superior Técnico, University of Lisbon,
Av. Rovisco Pais,
1049–001, Lisbon,
Portugal
E-mail: *hr@civil.ist.utl.pt*

Vicente S. Fuertes-Miquel
P. Amparo López-Jiménez
Hydraulic and Environmental Engineering Department,
Universitat Politècnica de València,
Camino de Vera, s/n. 46022, Valencia,
Spain

ABBREVIATIONS

A	area
C_d	discharge coefficient
C_{di}	intrusion discharge coefficient
d_{eq}	equivalent diameter
g	gravitational acceleration
h	head over the orifice
$N1$	exponent on equivalent FAVAD equation
P_w	wetted perimeter of the orifice
q_L	leakage flow
Q	flow
Re	Reynolds number
S	system expansion coefficient
v	flow velocity
$v_{intrusion}$	intrusion velocity
Δh	pressure head for intrusion flow

INTRODUCTION

Pathogen intrusion is a concern for the quality of drinking water in distribution networks. It may occur when the pressure inside the water pipe drops near a failure or leak; it allows the entrance of the external flow across the failure (Kirmeyer & Martel 2001). Pathogen intrusion (Figure 1) involves a combination of three factors: (1) a failure in a water pipe; (2) low or negative pressure in the pipe; and (3) saturated soil due to leaked water around the failure pipe. The external water accumulated by leaks could be polluted by diverse sources of pathogens (e.g., a sanitary sewer), and when the pressure drops inside the pipe, this external fluid could cause the pathogen intrusion. Although it is not common for all three factors to occur at once, it is a situation that could happen in present-day water distribution networks (Hunter *et al.* 2002; Karim *et al.* 2003; LeChevallier

doi: 10.2166/aqua.2015.121

Downloaded from https://iwaponline.com/aqua/article-pdf/64/8/857/399330/jws0640857.pdf
by guest

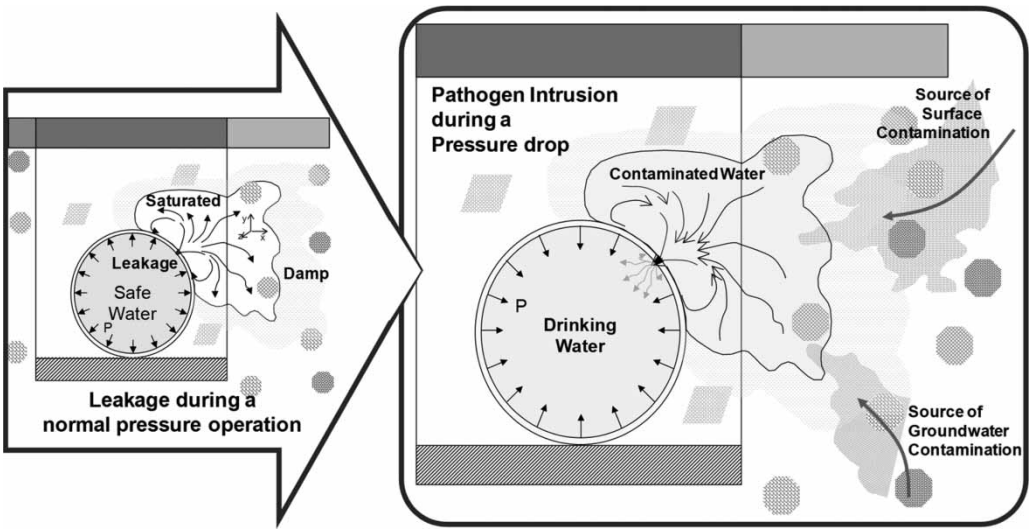

Figure 1 | Pathogen intrusion through a failure in pipes.

et al. 2003; Friedman *et al.* 2004; Pedley & Bartram 2004; Van Lieverloo *et al.* 2006; Ramalingam *et al.* 2009; Besner *et al.* 2010, 2011; Yang *et al.* 2011; Ebacher *et al.* 2012; Lee *et al.* 2012).

The failures in pipes depend on the pipe material, its age, the soil surrounding the pipe, water quality, water pressure and the pipe workmanship. The consequence of a failure is either a leak or an intrusion flow. The majority of the literature focuses on leaks. Pipe failures occur when environmental and operating conditions jeopardise the pipe structural integrity through corrosion, degradation, poor installation or manufacturing defects (Almeida & Ramos 2010). Rajani & Klein (2001) classified the types of failure into three categories: (1) circumferential breaks caused by longitudinal tension; (2) longitudinal breaks caused by cross-sectional tension (radial tension); and (3) cracks in joints caused by a cross-sectional tension. This classification must be complemented with additional breaks, such as holes due to corrosion (Mora-Rodríguez *et al.* 2011). Several authors (Rajani *et al.* 1996; Makar 2000; Lambert 2001; Rajani & Kleiner 2001; Hu & Hubble 2007; Silva *et al.* 2007; Clair & Sinha 2012; Haghighi *et al.* 2012) have studied the types of failure and their mechanisms.

The Fixed and Variable Area Discharge (FAVAD) theory and its variations have recently become one of the most commonly used theories to model pipe leakage (May 1994; Lambert 2001; Cassa & Van Zyl 2013, 2014; Van Zyl & Cassa 2014). Since the 1990s, diverse values of leakage flow at corresponding pressure have been found for different types of failure using this theory with diverse pipe materials such as metal and plastic, both in the laboratory and data from water district systems (Lambert 2001; López *et al.* 2007; Greyvenstein & Van Zyl 2007; Ávila & Saldarriaga 2011).

Intrusion has not received as much attention in the literature as leakage (Kirmeyer & Martel 2001; LeChevallier *et al.* 2003; Boyd *et al.* 2004a, b; McInnis 2004; López *et al.* 2008; Mora-Rodríguez *et al.* 2012, 2013, 2014; Yang *et al.* 2014). Authors such as Walski *et al.* (2006) and Collins & Boxall (2012) assert that the orifice equation quantifies the leakage and intrusion flows related to pipe failures, due to the relationship between flow and pressure through the orifice. Low or negative pressures in a distribution network are mainly caused by uncontrolled pump shutdowns, inadequate valve operation, network maintenance and the use of hydrants (Friedman *et al.* 2004).

A physical model of intrusion flow has been developed through different types of failure to evaluate the relationship between the intrusion flow and the head loss through the orifice. Owing to the pressure variation, the main failure section also varies, affecting the coefficients in FAVAD and orifice equations. Furthermore, the pathogen intrusion in porous soil is a little-studied topic in terms of experiments (Collins & Boxall 2012; Yang *et al.* 2014). In this paper, the experiments of the intrusion flow with and without porous

Downloaded from https://iwaponline.com/aqua/article-pdf/64/8/857/399330/jws0640857.pdf
by guest

media around pipes are analysed in order to better understand this phenomenon.

TYPES OF FAILURE

This section describes the representative types of failure in pipes used in the model: (1) round hole, (2) longitudinal split and (3) circumferential break (Rajani & Kleiner 2001).

Round holes

The orifice equation (Equation (1)) describes the rate of flow of liquid through an orifice. The magnitude of the round hole failures is determined according to this equation:

$$Q = C_d A(2g \cdot h)^{0.5} \tag{1}$$

where Q is the flow, A is the area of orifice, C_d is the discharge coefficient, g is the gravitational acceleration and h is the head over the orifice. The variables Q, h and C_d are obtained from diverse considerations related to the pipes and failures.

In 1994, May defined the FAVAD concept, which refers to the FAVAD. May assumed that the leak area is a linear function of pressure, which results in the following equation:

$$Q = C_d A(2g \cdot h)^{0.5} + C_d S(2g)^{0.5} \cdot (h)^{1.5} \tag{2}$$

where S is the system expansion coefficient.

Lambert (2001) presented an *N1* equation (Equation (3)) that is a generalisation of the orifice equation. The *N1* equation is obtained by fitting to data points before and after pressure management and then dividing one equation by the other. This equation is the most commonly used equation that relates the leak flow with pressure in the leak zone:

$$Q \text{ varies with } h^{N1} \text{ and } Q_1/Q_0 = (h_1/h_0)^{N1} \tag{3}$$

where *N1* is an exponent that may vary between 0.50 and 2.50, depending on the type of leak. The leakage flow (Q_1 and Q_0) and the pressure head inside the pipe (h_1 and h_0) are the data points before and after pressure management.

Similarly, the *N1* equation applied for longitudinal splits in plastic pipes postulates that the orifice area varies with pressure (Lambert 2001). If the split opens in one dimension, the exponent of the pressure in (Equation (3)) changes to 1.5 and if the split opens up in two dimensions (longitudinally and radially), the exponent of the pressure changes to 2.5. Furthermore, recent studies (Cassa & Van Zyl 2013; Van Zyl & Cassa 2014) have stated that this conventional power equation using *N1* does not provide a perfect representation of elastic leaks. These authors proposed a dimensionless leakage number that provides a more consistent characterisation. In future research, this new formula will be considered for representing leak behaviour in elastic materials.

The flow ranges used to determine the round hole diameter of the orifices are described in Table 1, according to the leakage classification proposed by McKenzie (1999), in relationship with its detection.

The head over the orifice (h) is considered in a range from 0 to −98.1 kPa, which are the limits that generate an intrusion into a pipe, without cavitation.

The discharge coefficient (C_d) varies with the Reynolds number (Lambert 2001). As indicated in Van Zyl & Cassa (2014), some models have been proposed to characterise the behaviour of orifice discharge coefficients, as Idelchik (1994) indicated. In particular, it is known that the C_d directly depends on the flow rate and diverse formulas can be considered for different orifice shape. For laminar flows (Reynolds numbers below 10), the relationship between flow rate and pressure head is linear, although for Reynolds numbers smaller than 1,000 this dependence already exists (Idelchik 1994).

Table 1 | Classification of leaks (based on McKenzie 1999)

Type of leak	q_L (m³/s)
Background leak and undetectable	$q_L < 2.8 \times 10^{-6}$
Background leak and difficult detection	$2.8 \times 10^{-6} < q_L < 5.5 \times 10^{-5}$
Reported leak and easy detection	$5.5 \times 10^{-5} < q_L < 1.4 \times 10^{-4}$
Reported leak	$1.4 \times 10^{-4} < q_L$

Downloaded from https://iwaponline.com/aqua/article-pdf/64/8/857/399330/jws0640857.pdf
by guest

A constant value is initially used to characterise pipe failures. Based on Lambert's (2001) experiments on round holes of 1 mm diameter and Reynolds number above 2,000, a C_d value of 0.75 was obtained. Nevertheless, drawing from other experiments diverse values of C_d have been found. For laminar flow, the C_d values were from 0.15 to 0.77; in transitional flow range, the C_d oscillates between 0.42 and 0.85; and in turbulent flow, the values obtained were from 0.56 to 0.74 (Lambert 2001; Yang *et al.* 2014). Some other authors have used constant values such as 0.60 (Ebacher *et al.* 2012), 0.70 and 0.80 (Lee *et al.* 2002, 2005), or obtained values between 0.71 and 0.76 (Walski *et al.* 2006). In another research project, the C_d values were specified according to the shape of the failure, 0.80 for a hole and 0.60 for a crack (Tabesh *et al.* 2009). The majority of the researchers relate the C_d to the Reynolds number. In this paper, the C_d is a calibration parameter at the end of the experiments.

According to the three variables (Q, h, C_d), diverse diameters were estimated for the experiments on pipe defects. The diameters, chosen according to the types of leak in the range of pressure mentioned above, are shown in Figure 2.

Four round holes failures with varying diameters were considered to simulate the intrusion flow and its relationship with the classification of leaks. In the case of the intrusion flow, according to the pressure range, the classification is proposed for two types of failure:

1. A large intrusion flow for round holes of 4.0 and 5.0 mm diameter represents the flow of a reported leak that is easy to detect.
2. A small intrusion flow for round holes of 1.0 and 1.5 mm diameter represents a flow for a background leak flow that is difficult to detect.

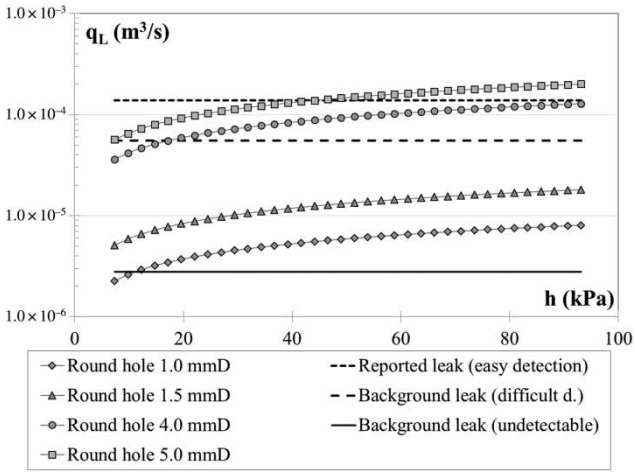

Figure 2 | Leakage flows through different round holes in a range 0–98.1 kPa.

Longitudinal splits and circumferential break

To determine the dimensions of longitudinal splits and circumferential breaks, the equivalent diameter equation proposed by Huebscher (Koch 2008) was used. For rectangular sections, Equation (4) was empirically obtained by considering the equivalent diameter of a circular section and the same pressure drop for an equivalent rectangular section. However, this empirical relationship has been questioned by Koch, since he obtained that the equivalent diameter for the rectangular duct is 4.5% smaller than the hydraulic mean diameter and the pressure drop could vary 26% for the same volume flow (Koch 2008). The equation of equivalent diameter proposed by Huebscher is used to obtain an equivalent diameter for designing the dimensions of the longitudinal splits and circumferential breaks that generate a similar flow through the round hole orifices for the same pressure drop. However, more experiments should be carried out in order to obtain a better understanding of the relationship between the equivalent diameter and the hydraulic mean diameter.

$$d_{eq} = 1.55 \cdot \frac{A^{0.625}}{P_w^{0.25}} \tag{4}$$

where d_{eq} is the equivalent diameter, A is the area of the orifice and P_w is the wetted perimeter of the orifice.

Based on Koch's research, Equation (4) was used to verify failure dimensions and to relate the longitudinal splits and circumferential breaks to the round holes. Two longitudinal splits and two circumferential breaks were built in the experimental device with a cutter (Figure 3). The PVC pipes were warmed to facilitate cutting. Upon cooling, the dimensions of the failures (Table 2) were obtained with a feeler gauge metric (approximately 0.05–1 mm). The mean average of the width and the area of failures were obtained reproducing the measurements in AUTOCAD© software.

The failure areas, which were obtained with equivalent diameters, are similar to the reported leaks (difficult

Downloaded from https://iwaponline.com/aqua/article-pdf/64/8/857/399330/jws0640857.pdf
by guest

Figure 3 | Longitudinal splits and circumferential breaks.

Table 2 | Size of longitudinal splits and circumferential breaks

Type of failure	Length (mm)	Width (mm)	A (mm^2)	d_{eq} (mm)	ID.
Large longitudinal split	44.5	0.135 (average)	6.30	1.6	LS44
Small longitudinal split	4.0	0.28	1.1	1.0	LS4
Large circumferential break	48.3	0.19 (average)	10.2	2.1	CB48
Small circumferential break	3.1	0.39 (average)	1.4	1.2	CB3

detection) in the pressure range shown in Figure 2. Therefore, the failures were similar to small round holes, according to the Huebscher equation, and the equivalent diameters obtained from a similar flow through the orifices showing the same pressure drop.

MODEL OF INTRUSION FLOW

The physical model consists of a pipe with a failure placed inside a tank that maintains a constant water level, which represents the source of external flow. With this model, the volume of water that can be introduced into the pipe was measured during a negative pressure event for the eight failures depicted in the section 'Types of failure'.

Set-up description

A physical model was built in the laboratory using controlled negative pressures in a pipe to generate different magnitudes of intrusion. The pressure was measured with a transducer with a range from −40 up to 80 kPa with an error >0.1%. The maximum power of the pump is 6 kW and a maximum flow of 90 litres per minute. The intrusion was simulated for steady-state conditions. The exterior volume of water was constant for all tests. The different parts of the

Downloaded from https://iwaponline.com/aqua/article-pdf/64/8/857/399330/jws0640857.pdf
by guest

experimental device for modelling the intrusion flow are shown in Figure 4(a). The model has two recirculation systems: the first recirculation system (Figure 4(b)) maintains the flow in the pipe (Figure 4(d)) and the second one (Figure 4(c)) maintains the water level over the pipe constant (Figure 4(e)). The pressure and flow data are registered in Figure 4(f) by using an interface in LabVIEW© software.

The intrusion flow originates from the second recirculation system to the first one. The intrusion flow was measured at a volumetric rate (Figure 5). The combination of the pump equipment downstream from the failure in the pipe and a partial closing of the valve upstream to the failure generates the negative pressure that allows the intrusion flow in the pipe.

The objective of the physical model was to verify the relationship between the pressure drop and the intrusion flow, analogous to the *N1* and orifice equations. Two different experiments were performed: the first one considers the pipe exterior without soil and the second one with soil. Below are the data and results of both experiments.

Experiments without soil around the pipe

The model PVC pipe is 32 mm nominal diameter and 2.4 mm thick and the inner diameter is 27.2 mm. The exterior tank had a constant water level of 0.37 m over the pipe. The negative pressure inside the pipe varied between −8.8 and −68.6 kPa. Depending on the type of failure, four to seven scenarios of negative pressure were simulated. The number of repetitions for each pressure scenario was the minimum required to establish the statistical significance. Seven to fifteen repetitions of each scenario were carried out to guarantee the results were consistent with a minimum error in the experimental data. Pressure scenarios and repetitions were randomly chosen. The process for these scenarios is described in Table 3.

This process was repeated to define the relationship between the intrusion flow and the negative pressure for each scenario. Tables 4 and 5 show a summary of each experiment carried out for the round holes, and the longitudinal splits and the circumferential breaks, respectively.

Experiments with soil around the pipe

Additional experiments were made considering soil around the pipe. The scenario was simulated with a circular hole leak of 1 mm diameter to generate the intrusion flow in a buried pipe. The granular material was fine gravel (Figure 6) not compacted.

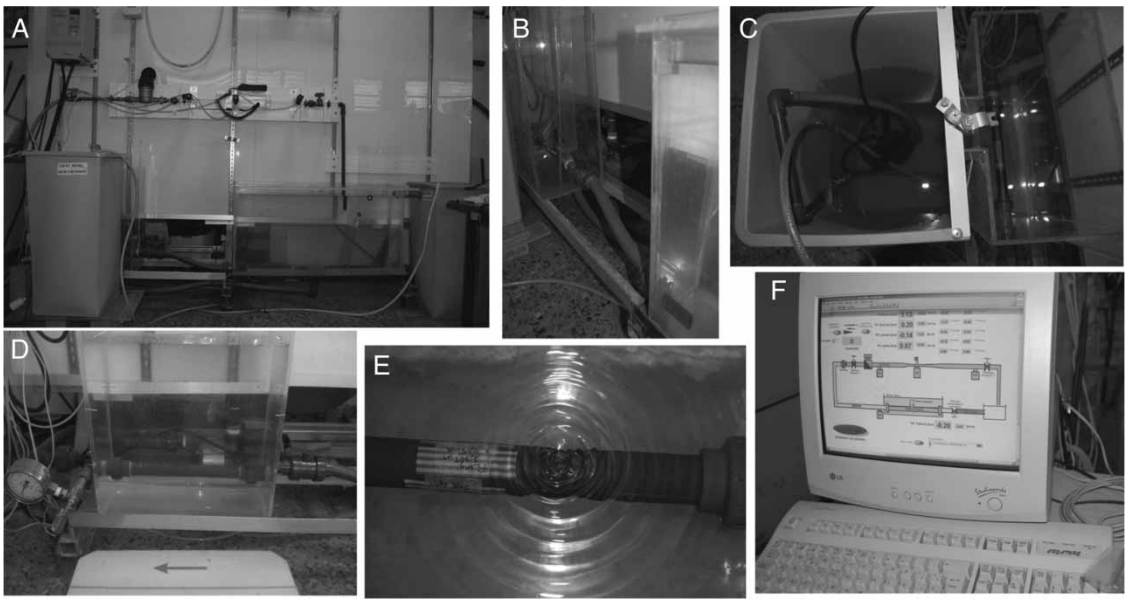

Figure 4 | Physical model and LabVIEW© software to control the system operation.

Downloaded from https://iwaponline.com/aqua/article-pdf/64/8/857/399330/jws0640857.pdf
by guest

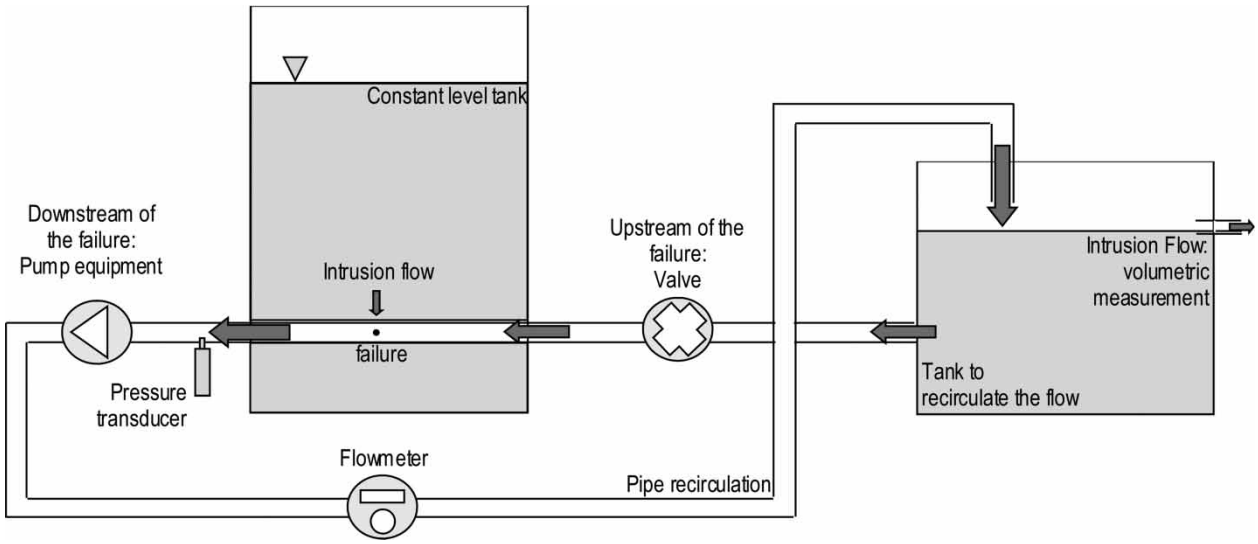

Figure 5 | Schema of the physical intrusion flow model.

Table 3 | Experiment procedure

Step	Description
1	To start the experiment, the pump equipment began and the valve upstream was partially closed to obtain a value of pressure between 0 and 98.1 kPa, according to the type of failure and the number of scenarios considered
2	The recirculation system of the intrusion tank was regulated based on the quantity of intrusion volume and on the type of failure in order to keep a constant water level and a low level of turbulence in the intrusion tank
3	After establishing a constant flow for the two recirculation systems, the pressure and the flow in the pipe were captured using LabVIEW© software and the intrusion flow was measured volumetrically

In these experiments, 88% of the external granular material had a diameter between 5 and 1.25 mm. The experimental process for this scenario was the same as described in Table 3. The results of pressure and intrusion flow were compared with the pipe with a round hole of 1 mm without porous media in the range of −13.7 to −51.0 kPa.

EXPERIMENTAL RESULTS

The results obtained for the diverse types of failure from the physical model are presented, first for experiments on intrusion flow without soil around the pipe and then for the experiments on intrusion flow with soil around the pipe.

Intrusion flow without soil around the pipe

The results were grouped into three groups. It was found in all cases that the intrusion flow without soil surrounding the pipe had an exponent value close to 0.5 (Figure 7).

Table 4 | Summary of round holes scenarios

Parameter	RH1	RH1.5	RH4	RH5
Number of scenarios	5	7	5	4
Repetitions	7	10	15	8
Max pressure (kPa)	−13.7	−10.8	−9.8	−22.6
Min pressure (kPa)	−51.0	−55.9	−33.3	−68.6
Min intrusion flow (m^3/s)	3.7×10^{-6}	6.8×10^{-6}	4.5×10^{-5}	4.8×10^{-5}
Max intrusion flow (m^3/s)	7.1×10^{-6}	1.5×10^{-5}	7.7×10^{-5}	1.6×10^{-4}

Downloaded from https://iwaponline.com/aqua/article-pdf/64/8/857/399330/jws0640857.pdf
by guest

Table 5 | Summary of longitudinal splits and circumferential breaks scenarios

Parameter	LS4	LS44	CB3	CB48
Number of scenarios	4	3	4	5
Repetitions	10	12	10	12
Max pressure (kPa)	−23.5	−14.7	−23.5	−8.8
Min pressure (kPa)	−58.8	−23.5	−52.0	−27.4
Min intrusion flow (m^3/s)	7.7×10^{-6}	9.6×10^{-7}	5.6×10^{-6}	6.7×10^{-5}
Max intrusion flow (m^3/s)	1.1×10^{-5}	1.6×10^{-6}	9.1×10^{-6}	1.3×10^{-4}

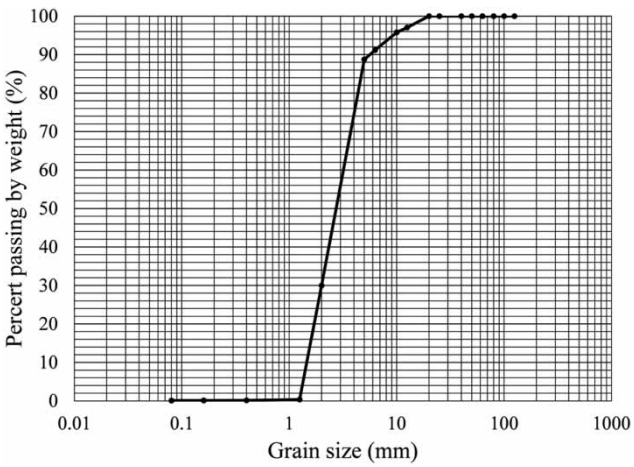

Figure 6 | Granulometric composition of the fine gravel.

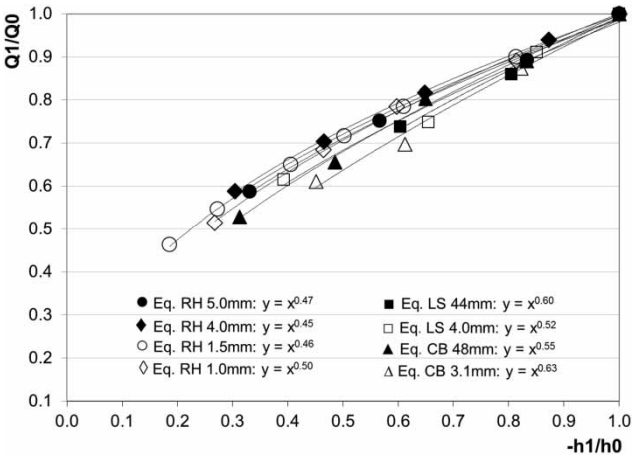

Figure 7 | *N1* equation applied for the diverse types of failure.

In the first group, the failures obtained exponent values under 0.5: the round holes of 4 mm (0.45), 1.5 mm (0.46) and 5 mm (0.47).

In the second group, the failures obtained exponent values near to 0.5: the round hole of 1 mm (0.50) and the longitudinal split of 4 mm (0.52).

In the third group, the failures obtained exponents with values higher than 0.50: the circumferential break of 48 mm (0.55), the longitudinal split of 44 mm (0.60) and the circumferential break of 3.1 mm (0.63).

The experimental results were adjusted to the potential equation and the coefficient of determination (R^2) was estimated in order to indicate how well experimental results fit to the potential equation. The round holes of 1, 1.5, 4.0 and 5.0 were the best fit (R^2 around 0.9986). Then, the circumferential break of 48 mm and the longitudinal split of 44 mm had an acceptable fit (R^2 around 0.9949). Finally, the circumferential break of 3.1 mm fitted with a coefficient $R^2 = 0.9857$ and the longitudinal split of 4 mm fitted with a coefficient $R^2 = 0.9754$.

The experimental results are adjusted in a form similar to the orifice equation (Equation (1)), in the following expression:

$$q_i = C(Dh)^{\exp} \tag{5}$$

In this case, the results fit acceptably well to a value of the exponent near to 0.5 (Figure 8). The exponential values are around 0.5 as they are the result of a numerical fitting. For the same negative pressure, the failures that provided higher flow were the circumferential break of 48 mm and the round holes of 5 and 4 mm. The failures that produced a medium flow were the round holes of 1.5 and 1 mm, the longitudinal split of 4 mm and the circumferential break of 3.1 mm. The failure that produced a small intrusion flow was the longitudinal split of 44 mm.

Downloaded from https://iwaponline.com/aqua/article-pdf/64/8/857/399330/jws0640857.pdf
by guest

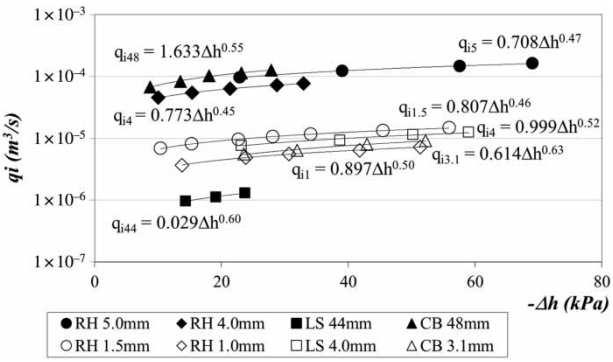

Figure 8 | Equation (5) for diverse failures.

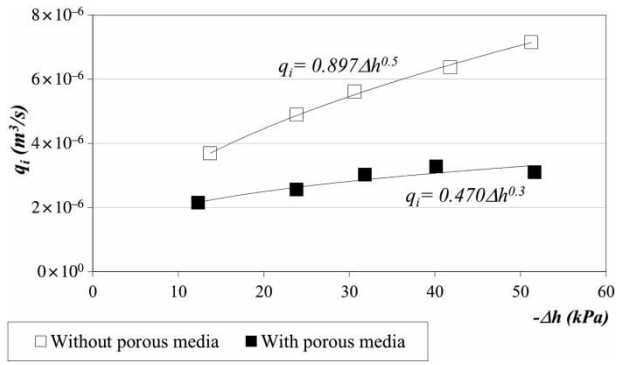

Figure 10 | Orifice equation with porous media for round hole of 1 mm.

Intrusion flow with soil around the pipe

The results of the intrusion flow and pressure are compared for the round hole of 1 mm without and with porous media. In this case, according to the *N1* equation (Figure 9), the exponent reduces its value from 0.50 to 0.30 when compared with the previous section.

According to the orifice equation, for the range of pressures from −10 to −55 kPa, the intrusion flow rate with the porous media represents a 52% average of the intrusion flow without the porous media (Figure 10), 64% for −10 kPa and 46% for the −55 kPa pressure.

In the case of the intrusion flow with porous media, fine gravel has an influence on the exponent, which decreases to 0.30. The presence of the porous media induces a resistance in the flow near the defect, as there is some fraction of water retention in the external media (White 2009). The property relating the porosity with the water retention in soils is the specific retention: the existence of pores in the external porous media provide for the passage or retention of water within the soil profile (Fetter 2001). This affects the flow passing across the holes in the intrusion process and therefore the exponent in the equation.

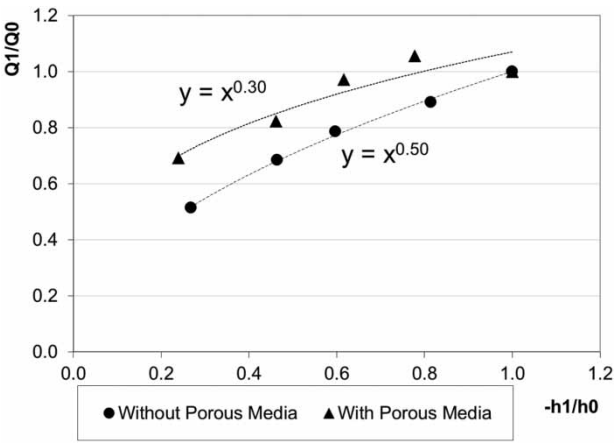

Figure 9 | *N1* equation with porous media for round hole of 1 mm.

ANALYSIS OF RESULTS: DISCUSSION

The experimental results for intrusion flow, modelled according to the *N1* and orifice equations, showed that some failures fit well according to the intrusion flow related to the leak classification.

1. Failures with maximum intrusion flow (between 0.20 and 0.40 m^3/h): circumferential break of 48 mm and round holes of 5 and 4 mm. These are similar to the flow of reported leak and easy detection.
2. Failures with medium intrusion flow (between 0.02 and 0.05 m^3/h): round holes of 1 and 1.5 mm, the longitudinal split of 4 mm and the circumferential break of 3 mm. According to the dimensions of the failures, the longitudinal split of 4 mm and the circumferential break of 3 mm have similar intrusion flows as the circular failures of 1 and 1.5 mm. The longitudinal and small circumferential failures obtained similar intrusion flows to that of the equivalent round holes. These intrusion flows are similar to background leak and difficult detection.

However, two failures did not obtain intrusion flows similar to the leak classification.

Downloaded from https://iwaponline.com/aqua/article-pdf/64/8/857/399330/jws0640857.pdf
by guest

1. The intrusion flow of the circumferential break of 48 mm was higher than the intrusion flow obtained with the equivalent diameter of 2.1 mm. In fact, this failure obtained higher intrusion flow than the round hole of 5 mm.
2. The longitudinal split of 44.5 mm was the failure that produced the smallest intrusion flow and was only obtained when negative pressure was close to zero. The intrusion flow was between 0.003 and 0.005 m^3/h, similar to the flow of an undetectable leakage. The flow obtained with the longitudinal split of 44 mm was 10 times smaller than the flow obtained with the equivalent diameter calculated of 1.6 mm.

In these cases, the large longitudinal and circumferential failures (LS44 and CB48) obtained different ranges of intrusion flows than the equivalent round holes, although the *N1* equation did not obtain values of the exponent superior to 0.60. In these two cases, the failure section variation must be considered in the equations to obtain the flows based on the orifice equation (Table 6).

The method used to verify the failure section variation was estimating a correction of the discharge coefficient for the longitudinal and circumferential failures. The correction is based on obtaining an equivalent discharge coefficient similar to the round hole sections that yield the same Reynolds number.

First, the intrusion discharge coefficient (C_{di}) of the round holes is calculated by Equation (6):

$$C_{\mathrm{di}} = \frac{Q}{A \cdot \sqrt{2 \cdot g \cdot \Delta h}} \tag{6}$$

where Q is the intrusion flow, A is the area of the orifice and Δh is the pressure head over the failure. Figure 11 shows the relationship between the C_{di} and the Reynolds number. Reynolds number is defined as the ratio between the product of mean velocity times diameter in the orifice, over the kinematic viscosity of water. As the flow across the failure changes, Reynolds number ranges from transitional up to turbulent flows. In this case, the range of the C_{di} is from 0.9 to 0.7. The value of the C_{di} diminishes with an increase in Reynolds number and the round hole diameter.

The Reynolds number for the flows through the large dimensions failures were estimated in order to obtain the values for validating the C_{di}. The intrusion velocity and the Reynolds number are calculated for the equivalent C_{di} for the longitudinal and circumferential failures in every scenario.

To obtain an equivalent C_{di}, the width of the longitudinal and circumferential failures is calibrated; and, consequently, the Reynolds number calculated is modified in order to verify the failure section variation with the correction of the discharge coefficient. Table 7 shows the equivalent C_{di} with the width proposed for both failures. The values of the C_{di} were proposed from the estimations obtained with the similar round hole that produced a similar intrusion flow. In the case of the LS44 failure, the intrusion flow is transitional. Therefore, based on Lambert's experiments, the C_{di} value obtained is close to 0.38 (Lambert 2001).

This method was implemented to quantify the variation of the failure area based on the numerical calibration of the C_{di} for large failures using the orifice equation. The area of intrusion could vary with the negative pressure. The flow variation of the last two failures (the circumferential break of 48 mm and the longitudinal split of 44 mm) could be affected by a variation in the failure's section during the

Table 6 | Reynolds number for the scenarios of negative pressure

Type of failure	D_{equiv} (mm)	Scenario	$V_{intrusion}$ (m/s)	Re	Regime
Large longitudinal split (LS 44)	1.6	1	0.15	244	Transition
		2	0.18	284	
		3	0.21	331	
Large circumferential break (CB 48)	2.1	1	6.6	13,937	Turbulent
		2	8.2	17,278	
		3	10.1	21,170	
		4	11.2	23,484	
		5	12.5	26,355	

Downloaded from https://iwaponline.com/aqua/article-pdf/64/8/857/399330/jws0640857.pdf
by guest

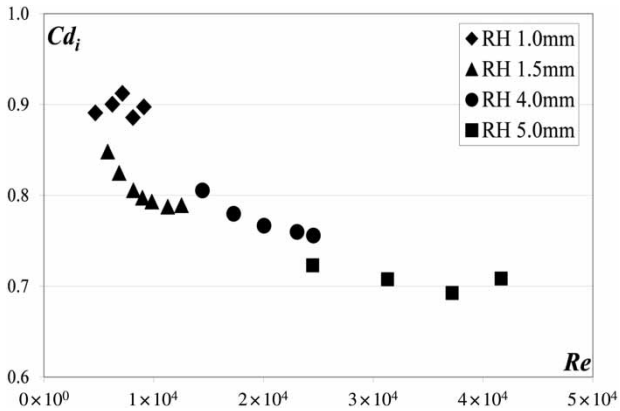

Figure 11 | C_{di} for round hole failures.

experiment. According to the methodology described and considering the C_{di} measured in the experiments, the section variation was modified to obtain the equivalent discharge coefficient (Table 8).

In the case of the longitudinal split, the negative pressure generated inside the pipe causes the section failure to practically close and the intrusion flow reaches values near to zero. On the other hand, the negative pressure inside the pipe caused the circumferential break to almost double its measured area.

CONCLUSIONS

This research dealt with modelling the intrusion flow in buried and unburied pipes. In particular, this work presented a method to perform experiments on a physical model in a steady-state according to the analogy of *N1* and orifice equations. The final objective was to obtain a contrasted set of equations to represent the relationship between intrusion flow across defects and negative pressure head in different sort of leaks.

Eight different failures were experimented on to represent equivalent flows for easy and difficult detection. One experiment was carried out with external porous media in order to simulate the conditions of the intrusion phenomenon on buried water distribution pipes. It was observed that the intrusion had been reduced to almost half of the flow when the scenarios were carried out with porous media around the hole in the range of pressure simulated.

The three types of failure obtained exponent values around 0.5 for the relationship of the pressure and intrusion flow. Although the large size longitudinal failure obtained a high intrusion flow in relation to its equivalent diameter, the exponent was still near to 0.5, similar to the orifice equation.

This work also proposed a method to quantify the variation of the width failure on longitudinal splits and on circumferential breaks. The method is based on determining the failure section variation by estimating a correction of the discharge coefficient. The correction proposed an equivalent discharge coefficient for each failure, similar to the round hole sections that yield the same Reynolds number. The results showed that the longitudinal failure practically closed during the intrusion, and the circumferential failures were opened to almost twice its area.

The topic of intrusion flow with soil around the pipe is quite new, and just recently documented. In this sense, this paper contributes to the relationships obtained, to implement in computational models of pipe networks. The characteristics of the porous media and its specific retention diminish the exponent of the *N1* equation. This information will allow modellers to quantify the potential volume of

Table 7 | Discharge coefficient for the longitudinal and circumferential failures

Type of failure	C_{di} objective	Thickness proposed (mm)	Scenario	New $V_{intrusion}$ (m/s)	New Re	C_{di} adjust
LS44	0.38	0.01	1	2.0	643	0.38
			2	2.4	754	0.38
			3	2.8	900	0.38
CB48	0.78	0.45	1	3.1	10,503	0.75
			2	3.9	13,020	0.75
			3	4.7	15,954	0.79
			4	5.3	17,697	0.77
			5	5.9	19,861	0.79

Downloaded from https://iwaponline.com/aqua/article-pdf/64/8/857/399330/jws0640857.pdf
by guest

Table 8 | Description of the variation of the area of the failure

Type of failure	Variation of the area of the failure (%)	Description of the variation
LS44	−93	Considering the equivalent C_{di}, the area could be almost closed. This is probably due to the failure length and its small width
CB48	+112	With the equivalent C_{di}, it shows that the calculated area is almost twice that of the area measured. The operating conditions of the negative pressure make this type of failure more vulnerable than others

external polluted water flow into pipes. With this knowledge, the model users and managers will have a very promising tool to estimate the potential risk and health implications of this phenomenon in real potable water systems.

ACKNOWLEDGEMENTS

DAIP-UG project 2013: 1101.31A02.42.205000 is acknowledged. The use of English in this paper was revised by the DAIP translation services (*Servicios de traducción del Departamento de Apoyo a la Investigación y al Posgrado*) of the University of Guanajuato.

REFERENCES

Almeida, A. & Ramos, H. 2010 Water supply operation: diagnosis and reliability analysis in a Lisbon pumping system. *J. Water Supply Res. T.* **59** (1), 66–78.

Ávila, H. & Saldarriaga, J. 2011 Parameter calibration leak longitudinal faults in PVC pipes. *Revista Científica Ingeniería y Desarrollo* **16** (16), 32–44 (in Spanish).

Besner, M. C., Ebacher, G., Jung, B. S., Karney, B., Lavoie, J., Payment, P. & Prévost, M. 2010 Negative pressures in full-scale distribution system: field investigation, modelling, estimation of intrusion volumes and risk for public health. *Drinking Water Eng. Sci.* **3** (2), 101–106.

Besner, M. C., Prévost, M. & Regli, S. 2011 Assessing the public health risk of microbial intrusion events in distribution systems: conceptual model, available data, and challenges. *Water Res.* **45** (3), 961–979.

Boyd, G. R., Wang, H., Britton, M. D., Howie, D. C., Wood, D. J., Funk, J. E. & Friedman, M. J. 2004a Intrusion within a simulated water distribution system due to hydraulic transients. I: description of test rig and chemical tracer method. *J. Environ. Eng-ASCE* **130** (7), 774–777.

Boyd, G. R., Wang, H., Britton, M. D., Howie, D. C., Wood, D. J., Funk, J. E. & Friedman, M. J. 2004b Intrusion within a simulated water distribution system due to hydraulic transients. II: volumetric method and comparison of results. *J. Environ. Eng-ASCE* **130** (7), 778–783.

Cassa, A. M. & Van Zyl, J. E. 2013 Predicting the pressure-leakage slope of cracks in pipes subject to elastic deformations. *J. Water Supply Res. T.* **62** (4), 214–223.

Cassa, A. M. & Van Zyl, J. E. 2014 Predicting the leakage exponents of elastically deforming cracks in pipes. In: *12th International Conference on Computing and Control for the Water Industry, CCWI2013. Procedia Engineering* **70**, 302–310.

Clair, A. M. & Sinha, S. 2012 State-of-the-technology review on water pipe condition, deterioration and failure rate prediction models. *Urban Water J.* **9** (2), 85–112.

Collins, R. & Boxall, J. 2012 Influence of ground conditions on intrusion flows through apertures in distribution pipes. *J. Hydraul. Eng.-ASCE* **139** (10), 1052–1061.

Ebacher, G., Besner, M. C., Clément, B. & Prévost, M. 2012 Sensitivity analysis of some critical factors affecting simulated intrusion volumes during a low pressure transient event in a full-scale water distribution system. *Water Res.* **46** (13), 4017–4030.

Fetter, C. W. 2001 *Applied Hydrogeology*. Prentice Hall, Upper Saddle River, NJ.

Friedman, M., Radder, L., Harrison, S., Howie, D., Britton, M., Boyd, G., Wang, H., Gullick, R., LeChevallier, M., Wood, D. & Funk, J. 2004 *Verification and Control of Low Pressure Transients in Distribution Systems*. AWWA Research Foundation, Denver, CO.

Greyvenstein, B. & Van Zyl, J. E. 2007 An experimental investigation into the pressure-leakage relationship of some failed water pipes. *J. Water Supply Res. T.* **56** (2), 117–124.

Haghighi, A., Covas, D. & Ramos, H. 2012 Direct backward transient analysis for leak detection in pressurized pipelines: from theory to real application. *J. Water Supply Res. T.* **61** (3), 189–200.

Hu, Y. & Hubble, D. W. 2007 Factors contributing to the failure of asbestos cement water mains. *Can. J. Civil Eng.* **34** (5), 608–621.

Hunter, P. R., Waite, M. & Ronchi, E. (eds) 2002 *Drinking Water and Infectious Disease: Establishing the Links*. CRC Press, Boca Raton, FL.

Idelchik, I. E. 1994 *Handbook of Hydraulic Resistance*. 3rd edn, Begell House, New York.

Karim, M. R., Abbaszadegan, M. & LeChevallier, M. 2003 Potential for pathogen intrusion during pressure transients. *J. Am. Water Works Ass.* **95** (5), 134–146.

Kirmeyer, G. J. & Martel, K. (eds) 2001 *Pathogen Intrusion into the Distribution System*. American Water Works Association, Denver, CO.

Downloaded from https://iwaponline.com/aqua/article-pdf/64/8/857/399330/jws0640857.pdf
by guest

Koch, P. 2008 Equivalent diameters of rectangular and oval ducts. *Build. Serv. Eng. Res. T.* **29** (4), 341–347.

Lambert, A. 2001 What do we know about pressure-leakage relationships in distribution systems. In *IWA Conference 'Systems approach to leakage control and water distribution system management'*. Brno, Czech Republic.

LeChevallier, M. W., Gullick, R., Karim, M., Friedman, M. & Funk, J. 2003 The potential for health risks from intrusion of contaminants into the distribution system from pressure transients. *J. Water Health.* **1**, 3–14.

Lee, J., Lohani, V. K., Dietrich, A. M. & Loganathan, G. V. 2012 Hydraulic transients in plumbing systems. *Water Sci. Technol.* **12** (5), 619–629.

Lee, P. J., Vítkovský, J. P., Lambert, M. F., Simpson, A. R. & Liggett, J. A. 2002 Leak detection in pipelines using an inverse resonance method. In: *Proc., May 2002 Conf. on Water Resources Planning and Management*. ASCE, Reston, VA.

Lee, P. J., Vítkovský, J. P., Lambert, M. F., Simpson, A. R. & Liggett, J. A. 2005 Leak location using the pattern of the frequency response diagram in pipelines: a numerical study. *J. Sound Vibration* **284** (3), 1051–1073.

López, P. A., Martínez-Solano, F. J., López-Patiño, G. & Lara-Ledesma, B. 2007 Computational model of the phenomenon of leaks in water supply pipes. *Ing. Hidraul. Mex.* **22** (2), 43–54 (in Spanish).

López, P. A., Mora, J. J., Pérez, R. & Martínez, F. J. 2008 Hydrodynamic modeling of the intrusion phenomenon in water distribution systems. *Ing. Hidraul. Mex.* **23** (4), 103–110 (in Spanish).

Makar, J. M. 2000 A preliminary analysis of failures in grey cast iron water pipes. *Eng. Fail. Anal.* **7** (1), 43–53.

May, J. 1994 Pressure dependent leakage. *World Water Environ. Eng.* **17** (8), 10.

McInnis, D. 2004 A relative-risk framework for evaluating transient pathogen intrusion in distribution systems. *Urban Water J.* **1** (2), 113–127.

Mckenzie, R. S. 1999 *Development of a standardized approach to evaluate burst and background losses in potable water distribution systems: SANFLOW User Guide.* South African WRC, Report TT 109/99.

Mora-Rodríguez, J., López-Jiménez, P. A. & Ramos, H. M. 2011 Intrusion problematic during water supply systems' operation. *Int. J. Energ. Environ.* **2** (3), 391–400.

Mora-Rodríguez, J., López-Jiménez, P. A. & Ramos, H. M. 2012 Intrusion and leakage in drinking systems induced by pressure variation. *J. Water Supply Res. T.* **61** (7), 387–402.

Mora-Rodríguez, J., Ramos, H. M. & López-Jiménez 2013 Pathogen intrusion events in drinking water distribution systems. *Tecnol. Cienc. Agua* **4** (3), 5–25.

Mora-Rodríguez, J., Delgado-Galván, X., Ramos, H. M. & López-Jiménez, P. A. 2014 An overview of leaks and intrusion for different pipe materials and failures. *Urban Water J.* **11** (1), 1–10.

Pedley, S. & Bartram, J. (eds.). 2004 *Pathogenic Mycobacteria in Water: A Guide to Public Health Consequences, Monitoring and Management*. IWA Publishing, London.

Rajani, B. & Kleiner, Y. 2001 Comprehensive review of structural deterioration of water mains: physically based models. *Urban Water* **3** (3), 151–164.

Rajani, B., Zhan, C. & Kuraoka, S. 1996 Pipe soil interaction analysis of jointed water mains. *Can. Geotech. J.* **33** (3), 393–404.

Ramalingam, D., Lingireddy, S. & Wood, D. 2009 Using the WCM for transient modeling of water distribution networks. *J. AWWA* **101** (2), 75–89.

Silva, R. C. C., Guerreiro, J. N. C. & Loula, A. F. D. 2007 A study of pipe interacting corrosion defects using the FEM and neural networks. *Adv. Eng. Softw.* **38** (11), 868–875.

Tabesh, M., Yekta, A. A. & Burrows, R. 2009 An integrated model to evaluate losses in water distribution systems. *Water Resour. Manage.* **23** (3), 477–492.

Van Lieverloo, J. H. M., Medema, G. & van der Kooij, D. 2006 Risk assessment and risk management of faecal contamination in drinking water distributed without a disinfectant residual. *J. Water Supply Res. T.* **55** (1), 25–31.

Van Zyl, J. E. & Cassa, A. M. 2014 Modeling elastically deforming leaks in water distribution pipes. *J. Hydraul. Eng.* **140** (2), 182–189.

Walski, T., Bezts, W., Posluszny, E. T., Weir, M. & Whitman, B. E. 2006 Modeling leakage reduction through pressure control. *J. Am. Water Works Ass.* **98** (4), 147–155.

White, R. E. 2009 *Principles and Practice of Soil Science: The Soil as a Natural Resource*. John Wiley & Sons, Malden, MA.

Yang, J., LeChevallier, M. W., Teunis, P. F. & Xu, M. 2011 Managing risks from virus intrusion into water distribution systems due to pressure transients. *J. Water Health* **9** (2), 291–305.

Yang, Y., Zhang, T. & Zhu, D. Z. 2014 Influence of porous media on intrusion rate into water distribution pipes. *J. Water Supply Res. T.* **63** (1), 43–50.

First received 7 September 2014; accepted in revised form 6 May 2015. Available online 18 June 2015

Downloaded from https://iwaponline.com/aqua/article-pdf/64/8/857/399330/jws0640857.pdf
by guest